agronomy

MDPI

Article

Design of an Agrivoltaic System with Building Integrated Photovoltaics

Sojung Kim [1] and Sumin Kim [2,*]

[1] Industrial and Systems Engineering, Dongguk University-Seoul, Seoul 04620, Republic of Korea; sojungkim@dgu.ac.kr
[2] Department of Environmental Horticulture & Landscape Architecture, College of Life Science and Biotechnology, Dankook University, Cheonan-si 31116, Chungnam, Republic of Korea
* Correspondence: sumin.kim@dankook.ac.kr; Tel.: +82-41-550-3644

Abstract: Building integrated photovoltaics (BIPVs) are becoming popular as building elements such as windows, roofs, and outer walls. Because BIPVs have both a construction material function and an electricity generation function, they are a promising alternative to sustainable buildings. This study aims to propose a novel agrivoltaic system design that produces crops underneath photovoltaic (PV) modules. Regarding the fact that crop growth is significantly influenced by shading from PV modules, roof BIPVs with different shading ratios can lead to increased crop productivity. Thus, BIPV design should be investigated based on the performance estimation and feasibility evaluation of different shading ratios in an agrivoltaic system. To this end, electricity generation and crop production models are devised by polynomial regression (PR) based on field experiment data collected from the agrivoltaic system at the Agricultural Research Service Center in Naju-si, South Korea. The experiment shows that a shading ratio of 30% allows for the maximization of the profitability of electricity and soybean production in an agrivoltaic system equipped with BIPVs. As a result, this research will contribute to implementing an agrivoltaic system with various BIPVs.

Keywords: building integrated photovoltaics; agrivoltaic; photovoltaic; renewable energy; soybean

Citation: Kim, S.; Kim, S. Design of an Agrivoltaic System with Building Integrated Photovoltaics. *Agronomy* **2023**, *13*, 2140. https://doi.org/10.3390/agronomy13082140

Academic Editor: Miguel-Ángel Muñoz-García

Received: 18 July 2023
Revised: 9 August 2023
Accepted: 15 August 2023
Published: 16 August 2023

1. Introduction

For decades, photovoltaics (PVs) have been used as a popular material for generating electricity from renewable energy source (i.e., solar energy) [1]. The global movement to reduce greenhouse gas (GHG) emission [2] has become a more popular material in renewable energy production. Because PVs can be attached to a wall and a roof, they have the potential to be used as building element, in a system which is also known as building integrated photovoltaics (BIPV) [3]. Considering that buildings consume 30% of global energy, using PVs as building elements can mitigate GHG emissions [4]. Accordingly, the levelized cost of electricity (LCOE) of a roof top BIPV system is only 72% of the LCOE of a green roof system in Texas, USA [5]. Hence, it is a profitable alternative to implement the concept of green buildings. Notice that a green roof (or a vegetation roof) is another well-known option for thermal and energy efficient buildings [6].

The most significant advantage of BIPVs is renewable energy production, but BIPVs also have other benefits [7]. For example, BIPVs reduce air conditioner use in a building in summer because the PV cells in BIPVs can block the excessive solar radiation from windows [8]. In addition, the warranty duration of PV modules is between 20 and 25 years. Therefore, BIPVs are highly reliable in the long term [9]. The thickness and strength of BIPV involving PV cells made of c-Si, a-Si, or CdTe PV cells provide better thermal insulation and acoustic insulation functions than windows [10]. Due to the multiple benefits of BIPVs, their global market value was 19.82 billion U.S. dollars in 2022, and the compound annual growth rate from 2023 to 2030 is expected to be 21% [11].

Nevertheless, the electricity productivity of BIPVs (i.e., semi-transparent BIPVs) is lower than conventional PVs because of their installation positions and the number of installed PV cells in a BIPV panel. In fact, when the incident angle of solar radiation is above 45°, the conversion efficiency is significantly reduced [12]. It implies that BIPVs used as windows may not have sufficient productivity in electricity generation. Unlike a regular PV, a semi-transparent BIPV consists of resin, glasses, and PV cells so that some transparent areas of a BIPV cannot generate electricity [13]. This limited capability in electricity generation may delay technology diffusion in building construction.

There exists a new application of a BIPV in the field of agriculture. It is an agrivoltaic system that harvests crops underneath PVs [2]. Since the harvest yields of crops are influenced significantly by the shade of PVs in the system, it is critical to set an appropriate shading ratio to maximize productivity in crop production and electricity generation [14]. To this end, the decision support system (DSS) for dynamic performance evaluation of an agrivoltaic system was devised [15]. However, observing that a BIPV is flexible to adjust its design (i.e., PV cell arrangement), it provides a control function of a shading ratio of an agrivoltaic system. In other words, the shading ratio can change after the construction of the system. Therefore, farmers can replace BIPVs with an appropriate shading ratio to maximize their profits when crops change due to market values.

This study aims to introduce a framework identifying the best design of an agrivoltaic system integrated with BIPVs in terms of its economic value. Semi-transparent BIPVs, which can send solar radiation underneath BIPVs, are considered a roofing material of an agrivoltaic system (see Section 2.1 for more detail). In order to design the system, the performance of electricity generation and soybean production under different shading ratios were evaluated and estimated. The data collected from the Agrivoltaic system located at the Jeollanam-do Agricultural Research and Extension Services in Naju-si (35.0161° N, 126.7108° E), Jeollanam-do, South Korea, were used to build the performance estimation models. Polynomial regression (PR) is adopted to develop estimation models, which enable the capture of nonlinear relationships between independent and dependent variables [16]. In addition, the optimization model is devised to identify the best shading ratio of BIPV with the maximum profit, and the selected shading ratio is used to design a semi-transparent BIPV installed on a roof of an agrivoltaic system. As a result, the proposed framework will contribute to the implementation BIPVs in agrivoltaic systems.

The rest of the paper is organized as follows. Section 2 summarizes studies about roof BIPVs and agrivoltaic systems and explains the agrivoltaic system design with BIPVs based on the estimation of electricity generation and crop production. Section 3 illustrates the identification process of the optimum BIPV design in terms of the economic value of an agrivoltaic system. Section 4 will conclude the study and findings.

2. Materials and Methods

2.1. Roof Building Integrated Photovoltaics for Agrivoltaic Systems

As mentioned in Section 1, BIPVs are PV modules used as building elements [3]. Although there are multiple types of BIPVs, such as an outer wall, a roof, and windows [7], this study focuses on roof BIPVs, which can be used in an agrivoltaic system. Figure 1 represents the Agrivoltaic system at the Jeollanam-do Agricultural Research and Extension Services in Naju-si (35.0161° N, 126.7108° E), Jeollanam-do, South Korea.

Agrivoltaic systems have been studied in multiple countries such as Germany, Japan, China, United States, France, Chile, and South Korea [14,17–19]. In particular, it is beneficial for countries with land shortage problems, as it simultaneously utilizes the limited land resources to produce electricity and crops [2]. Accordingly, the agrivoltaic system preserves moisture and organic matter in the soil, which results in water use reduction [20].

However, because PV modules in an agrivoltaic system create shade, crop harvest yields may differ from those produced from regular farms in open fields. In fact, according to the field study conducted to understand the shading impact on the yield of crops (e.g., sesame, mung bean, red bean, corn, and soybean) [2], the yield of five crops were decreased to 30–53% at a shading ratio of 32%. Nevertheless, due to the revenue from electricity production through PV modules, the agrivoltaic system eventually contributes to increase the income of farmers.

(a) (b)

Figure 1. The agrivoltaic system in South Korea: (**a**) crops underneath photovoltaic modules; (**b**) photovoltaic modules.

The roof BIPV has three different classifications: (1) PV modules on a rooftop [21]; (2) PV modules attached to a roof [22]; and (3) PV modules integrated in a roof (or a greenhouse roof) [23]. Figure 2 illustrates three different types of roof BIPVs.

(a) (b) (c)

Figure 2. The roof building integrated photovoltaics (BIPVs): (**a**) rooftop PVs; (**b**) roof attached PVs; and (**c**) roof integrated PV.

PV modules on a rooftop (i.e., rooftop PVs) are traditional rooftop PVs taking 80% of the BIPV market [3]. The PV modules attached to a roof (i.e., roof attached PVs) are a popular design for the individual household because they do not change any existing roof design and require additional cost to construct pillars to support PV modules. The PV modules integrated into a roof (i.e., roof integrated PVs) are novel alternatives to substitute building elements. Although the strength and durability of roof integrated PVs are relatively weaker than those of a roof made of cement and brick, they are appropriate alternatives for a thin roof made of glasses [8]. For example, they can be used as a roof for a nursery in agriculture because they do not block all solar radiation needed for crop production. Figure 3 illustrates the structure of a semi-transparent BIPV [24]. Unlike traditional PV modules, solar radiation can penetrate the semi-transparent BIPV.

Suppose the semi-transparent BIPV is used as a roof integrated PV for an agrivoltaic system. In that case, the shading ratios of the system can be reduced, which improves crop production. In an agrivoltaic system, the distance between the pillars supporting the PV modules primarily affects the shading ratio. However, using roof integrated PVs provides another opportunity to easily control shading ratios by changing the design of semi-transparent BIPVs.

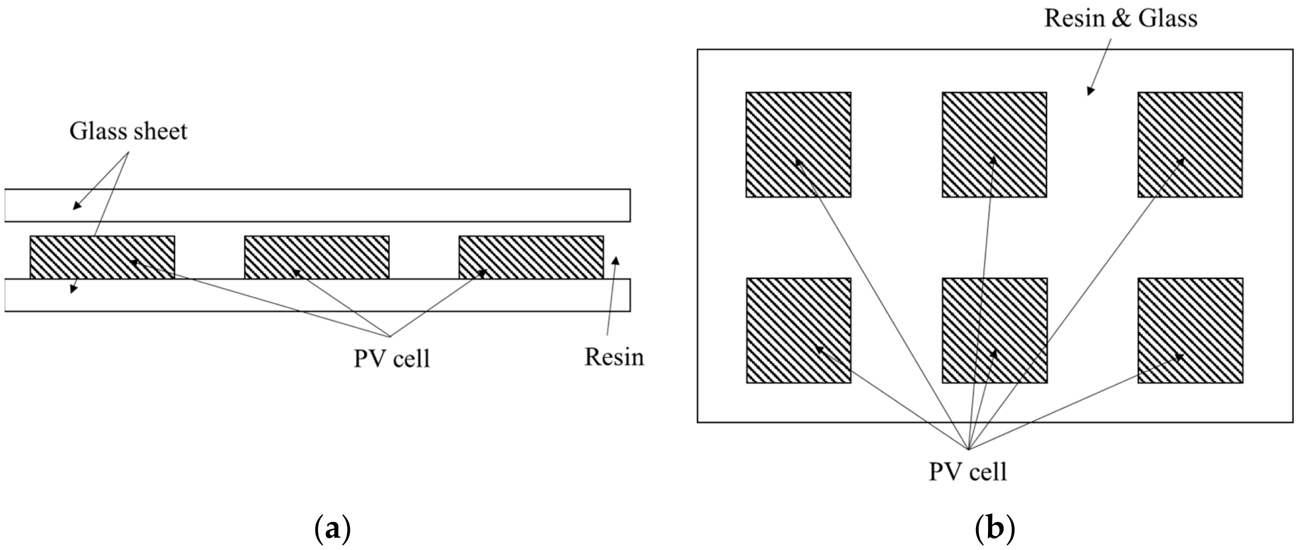

Figure 3. Structure of a semi-transparent building integrated photovoltaic (BIPV): (**a**) side view; (**b**) front view.

2.2. Design of an Agrivoltaic System with Building Integrated Photovoltaics

This study proposes a design framework for an agrivoltaic system integrated with BIPVs. Figure 4 illustrates the proposed framework with seven stages. Once a structure of the agrivoltaic system is determined, the BIPV design must be selected. However, there is a significant correlation between a shading ratio and BIPV design, and an appropriate shading ratio should be determined. To this end, the performance of an agrivoltaic system in terms of electricity generation quantity and crop production yield is estimated. The estimated performance is transformed to economic value in the feasibility analysis stage. This process continues until the optimum shading ratio is found. After that, the framework designs a BIPV under the selected shaded ratio. The following sections provide the primary stage in detail.

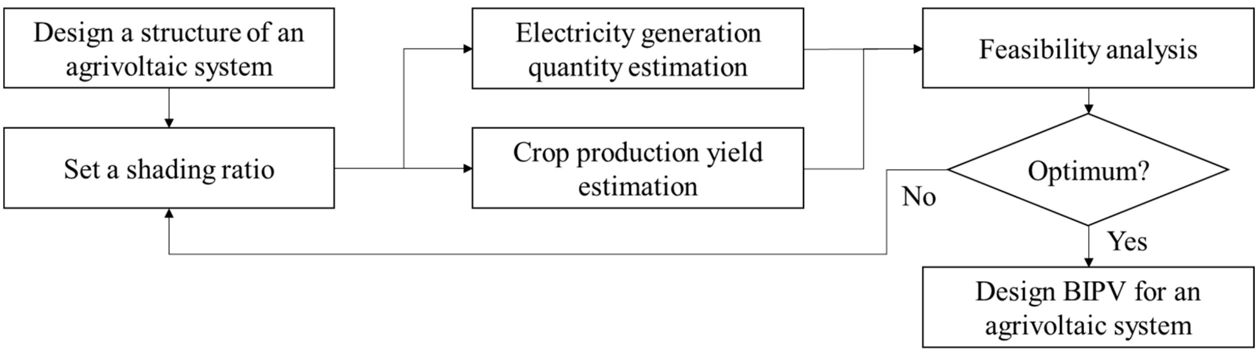

Figure 4. Proposed framework for agrivoltaic system design with building integrated photovoltaics.

2.2.1. Electricity Generation Quantity Estimation

Figure 4 shows the electricity generation quantity by BIPV estimated through polynomial regression (PR). This popular machine-learning technique captures the correlation between independent and dependent variables through their coefficients [16]. The PR model is described in Equations (1) and (2) [5].

$$Y = g(X_1, \ldots, X_n) = \beta_0 + f_1(X_1) + \ldots + f_n(X_n) + \varepsilon,\ \varepsilon \sim N\left(0, \sum_{j=1}^{n} \sigma_j^2\right) \quad (1)$$

$$f_j(X_j) = \beta_{j1}(X_j) + \beta_{j2}\left(X_j^2\right) + \ldots + \beta_{jL}\left(X_j^L\right),\ j = 1,\ 2,\ \ldots,\ n \tag{2}$$

where $f_j(X_j)$ is the polynomial function of variable X_j; $\beta_0 = \sum_{j=1}^{n} \beta_{j0}\left(X_j^0\right)$; $X_j^0 = 1$; β_j is a coefficient of X_j; and β_0 is the constant term. In Equations (1) and (2), the least squares method is used to identify coefficients of variables. According to [4], electricity generation ($E_{PV}(S)$, kWh/m^2/day) by monofacial PVs can be explained with seven variables as follows: (1) X_1: daily solar radiation (MJ/m^2); (2) X_2: maximum daily temperature (°C); (3) X_3: minimum daily temperature (°C); (4) X_4: daily precipitation (mm); (5) X_5: daily humidity (%); (6) X_6: daily wind speed (m/s); and (7) S: shading ratio ($0.20 \leq S \leq 0.32$). Equation (2) represents the estimation model of electricity generation.

$$\begin{aligned} E_{BIPV}(S) = -5.42 \quad & \times 10^{-2} + 1.75 \times 10^{-2} X_1 - 1.07 \times 10^{-17} X_2 + 4.73 \times 10^{-19} X_3 \\ & + 1.97 \times 10^{-19} X_3^2 - 4.88 \times 10^{-19} X_4 + 1.00 \times 10^{-21} X_4^2 \\ & + 3.29 \times 10^{-18} X_5 - 3.18 \times 10^{-22} X_5^3 + 2.86 \times 10^{-18} X_6 \\ & + 2.06 \times 10^{-1} S \geq 0 \end{aligned} \tag{3}$$

Notice that Equation (3) estimates an electricity generation quantity regarding climate variables having a non-linear relationship with $E_{BIPV}(S)$. Regarding the coefficient of shading ratio S, there is a positive correlation between a shading ratio and electricity generation quantity.

Table 1 describes the yield estimation model of Soybean production devised under different shading ratios based on the field study data. In 2020, soybean (*Glycine max*) was planted and harvested from June to October at the Jeollanam-do Agricultural Research and Extension Services (35.0161° N, 126.7108° E), located in Naju-si, South Korea [2]. The average temperature and total rainfall were 23.55 °C and 1477.9 mm, respectively. Accordingly, in the experiment, the reduction ratios from the yield of the open field (0% shading ratio) were −13%, −21%, and −30%, respectively.

Table 1. Harvested yields of soybean under four different shading levels (0, 21.3, 25.6, and 32%) (edited from [2]).

Crop Type	Shading Levels (%)			
	0	**21.3**	**25.6**	**32**
Soybean (kg/ha)	3640	3150	2880	2540

2.2.2. Crop Production Yield Estimation

Equation (4) represents the yield estimation model of soybean.

$$Y_{soybean}(S) = 3640 - 318S - 9868S^2 \geq 0 \tag{4}$$

where S is a shading ratio ($0 \leq S \leq 0.32$). The coefficient of determination (R^2) of Equation (4) is 99.72% so that the developed model can accurately estimate soybean yields under different shading ratios. In Figure 5, the harvest yields nonlinearly decrease as the shading ratio increases. Regrading the fact that the quantity of electricity generation increases as the shading ratio increases, this nonlinear relationship conflicts with the quantity of electricity generation. It implies that a farmer must determine the optimal shading ratio which produces electricity without causing harmful impact on the production yield of a crop.

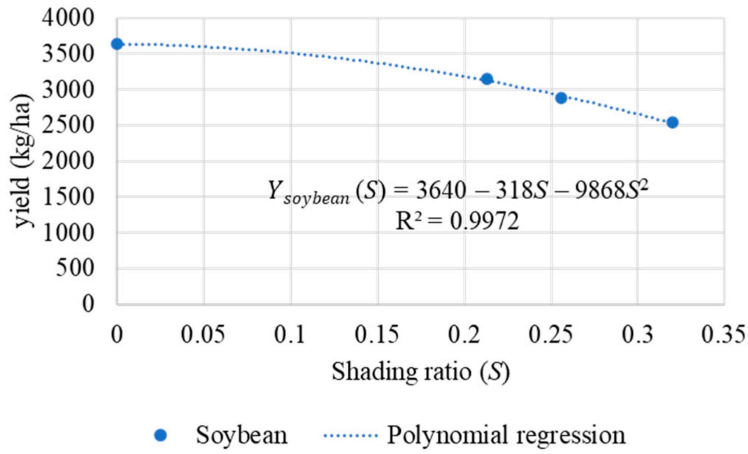

Figure 5. Harvest yields of soybean under different shading ratios.

2.2.3. Feasibility Analysis and Shading Ratio Determination

The estimation models of electricity generation and soybean production can be used to identify the best shade ratio of BIPV with maximum profit of Z in Equation (5).

$$Max\ Z = f_{electricity}(S) + f_{soybean}(S) \tag{5}$$

subject to

$$f_{electricity}(S) = \beta_{BIPV}E_{BIPV}(S) - \gamma_{BIPV}E_{BIPV}(S) \tag{6}$$

$$f_{soybean}(S) = \beta_{soybean}Y_{soybean}(S) - \gamma_{soybean}Y_{soybean}(S) \tag{7}$$

$$Y_{soybean}(S) \geq Y_{soybean,\ min} \tag{8}$$

$$0 \leq S \leq 0.32 \tag{9}$$

where S is the shading ratio generated by BIPV; β_{BIPV} is the unit price of electricity sales; γ_{BIPV} is the unit production cost of electricity; $\beta_{soybean}$ is the selling price of soybean; $\gamma_{soybean}$ is the unit production cost of soybean; $f_{electricity}(S)$ is the profit function subtracting the production cost of electricity from the total revenue of electricity generation; $f_{soybean}(S)$ is the profit function subtracting the production cost of soybean from the total revenue of soybean; and $Y_{soybean,min}$ is the minimum required yield of soybean. Notice that an agrivoltaic system aims to generate electricity without affecting food security issues. Therefore, the minimum required yield of a crop should be considered in its design.

3. Results and Discussion

3.1. Scenario

The proposed performance estimation framework was used to design an agrivoltaic system consisting of roof integrated BIPVs. Figure 3 shows the semi-transparent BIPV used on the roof of an agrivoltaic system. Figure 6 reveals the structure of the agrivoltaic system considered in this study.

In Figure 6, e_1 is the horizontal distance of an area shaded by a BIPV; e_2 is the horizontal distance of the open area between BIPVs; q is the length of a BIPV; ω is the solar altitude angle (°); τ is a tilt angle of a BIPV(°). The value of e_1 is calculated by Equation (10).

$$e_1 = q\cos(\tau) \tag{10}$$

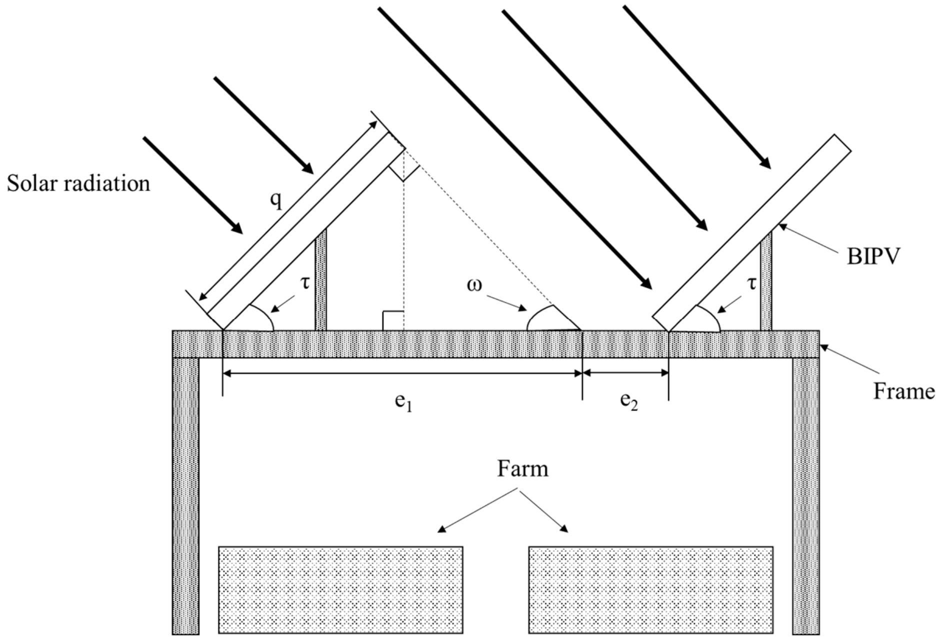

Figure 6. Design of the subject agrivoltaic system.

According to theory [25], ω should be the solar altitude angle at noon to maximize the productivity of BIPVs, and it should be $45° \leq \omega \leq 90°$. In South Korea, most PV modules have a tilt angle (τ) of 30° to maximize the productivity of PVs [26]. Regarding both conditions, e_1 should be between q and $2q/\sqrt{3}$. In other words, when $e_2 = 0$, the shading ratio (S) can be between 86.6% and 100% according to Equation (11).

$$S = q/(e_1 + e_2) \tag{11}$$

However, in this condition, crops underneath BIPVs cannot grow due to the high shading ratio, so an additional distance between the BIPVs (e_2) must be considered. According to [2], the maximum shading ratio of 32% is required for the agrivoltaic crop production system. Thus, this study assumes the maximum shading ratio of 32% to meet the soybean's minimum production quantity (0.25 kg/m^2). In other words, e_2 should be greater than 1.9 q when $e_1 = 2q/\sqrt{3}$.

Table 2 describes the climate data of the subject area (i.e., the Agricultural Research Service Center in Naju-si, South Korea) from 2012 to 2022 [27]. Note that the crop growing season from June to October generally has higher solar radiation values than other months. This results in higher productivity in terms of electricity generation. The daily average solar radiation, surface temperature high, surface temperature low, precipitation, humidity, and wind speed are 2.14 MJ/m^2, 18.22 °C, 10.91 °C, 97.29 mm, 77.68%, and 3.32 m/s, respectively. The data are used to estimate the electricity generation quantities of a roof integrated BIPV.

The system marginal price (SMP) and renewable energy certificate (REC) are considered to calculate the electricity revenue produced. The SMP and REC are USD 0.12/kWh and USD 0.05/kWh in south Korea in 2023, respectively [28]. The electricity production costs are estimated based on the data in Table 3. According to [29], BIPVs are 1.46 times more expensive than regular PV modules due to their customized design. The lifetime of PV is assumed to be 25 years regarding the warranty duration of PVs [30].

Table 2. Observed daily climatic data from 2012 to 2022 [27].

Month	Solar Radiation (MJ/m^2)	Surface Temperature High (°C) [1]	Surface Temperature Low (°C) [2]	Precipitation (mm)	Humidity (%)	Wind Speed (m/s)
January	1.54	5.40	−1.31	32.93	74.55	3.76
February	1.84	6.75	−0.65	29.31	72.64	4.06
March	2.12	12.18	3.47	76.54	74.27	3.76
April	2.34	17.37	8.77	96.46	73.64	3.45
May	2.52	22.61	13.89	83.69	75.82	3.05
June	2.85	25.86	19.15	116.38	83.00	2.67
July	2.89	28.97	23.27	213.89	87.27	2.93
August	2.48	30.45	24.26	181.65	84.18	2.90
September	2.30	26.25	19.26	153.35	81.55	2.65
October	1.85	20.95	13.16	82.07	75.36	3.21
November	1.56	14.34	7.00	55.82	74.80	3.51
December	1.44	7.54	0.65	45.42	75.10	3.89

[1] The highest air temperature; [2] the lowest air temperature.

Table 3. Construction, operating, and maintenance costs of an APV system.

Data Type	21.3%	25.6%	32%
Solar module cost (USD/m^2) [1]	6.38	6.81	9.19
Structure cost (USD/m^2)	7.24	7.72	10.43
Electric distribution system cost (USD/m^2)	3.45	3.68	4.97
Other costs (USD/m^2) [2]	0.25	0.27	0.36
Total Construction cost (USD/m^2)	17.32	18.48	24.95
Annual operating and maintenance costs ($USD/m^2/year$) [3]	0.59	0.71	0.89

[1] the cost is estimated from the market price of BIPV [29]; [2] The costs include the building permit fee and the fee for linkage to the existing electric distribution system; [3] the cost estimates from [31].

The total construction costs (the present values) are transformed into annual values via Equation (12) under the given discount rate of r. It is known as the equal-payment-series capital-recovery factor [32].

$$A = P\left[\frac{r(1+r)^n}{(1+r)^n - 1}\right] \tag{12}$$

where A is the annual worth (USD); P is the present worth (USD); and n is the lifetime of a BIPV (year). As a result, the annual cost of electricity generation computes to include investment (i.e., construction), operating, and maintenance costs.

Table 4 describes soybean production cost involving material, labor, and overhead costs. The total production cost is USD $0.56/m^2/year$. According to [33], the selling price of soybean in 2022 is USD 5.68/kg. The profitability of electricity under given costs and sales data and crop production under different shading ratios are used in Section 3.2.

Table 4. Production cost of soybean.

Crop Type	Material Cost (USD)				Labor Cost (USD)	Overhead Cost (USD)
	Seed	Fertilizer	Pesticides	Other		
Soybean ($USD/m^2/year$)	0.16	0.04	0.02	0.02	0.03	0.29

3.2. Identification of the Best Shading Ratio for an Agrivoltaic System

The best shading ratio of a roof integrated BIPV at the subject agrivoltaic system is identified through Equation (5), shown in Section 2.2.3. From the given climate data in Table 2, the daily electricity generation quantities ($E_{PV}(S)$, kWh/m^2/day) of PV modules are initially estimated. Figure 7 illustrates the estimated results. As the shading ratio increases, more PV modules can be installed within a unit area (m^2) to increase electricity generation quantities. In Figure 7, the crop growing period from June to October has the highest productivity due to climate characteristics described in Table 2.

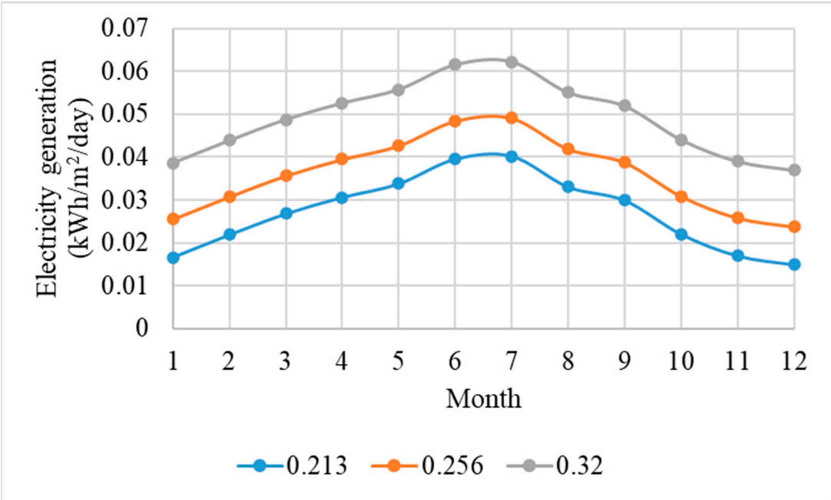

Figure 7. Electricity generation quantities under different shading ratios.

Figure 8 represents the annual revenue, cost, and profit of electricity generation under two cases, such as the REC and SMP case and the SMP case. As mentioned in Section 3.1, the electricity sales price in the REC and SMP case is USD 0.17/kWh, and the sales price in the SMP case is USD 0.12/kWh. Notice that a discount rate of 0.05 is considered in both cases. In the case of REC and SMP, there is a positive profit when the shading ratio is more significant than and equal to 0.23. In other words, if the shading ratio is lower than 0.23, there is no profit due to high production costs involving the construction, operating, and maintenance costs. Under the SMP case, there is no positive profit under all the shading ratios. This implies the significance of REC in making a positive profit from electricity sales generated by BIPVs.

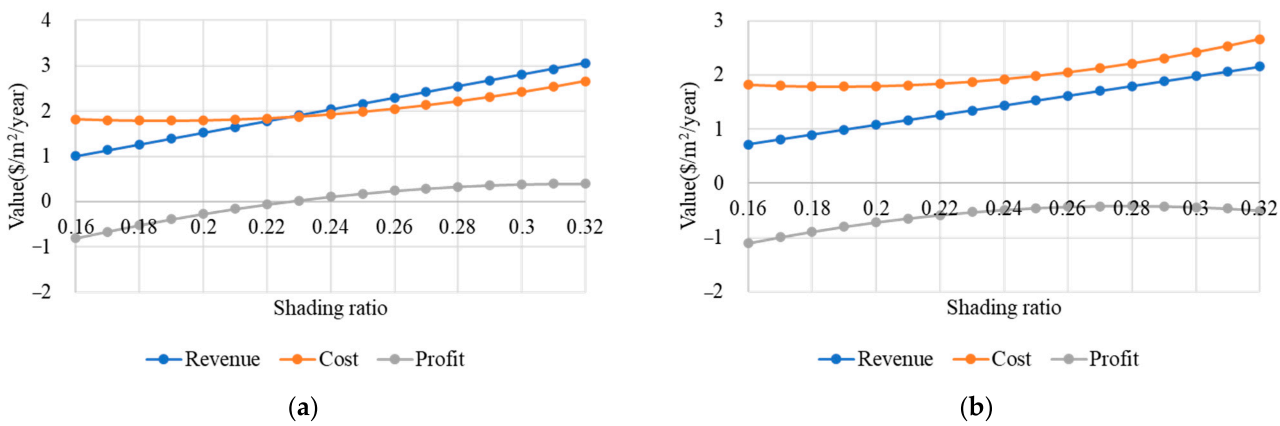

Figure 8. Revenue, cost, and profit of electricity generation: (**a**) REC and SMP case; (**b**) SMP case.

On the other hand, in Figure 9, profit from crop production nonlinearly decreases as the shading ratio increases. The profit becomes the minimum value of USD 0.49/m^2 at the shading ratio of 32%. Notice that the required minimum production quantity of soybean is 0.25 kg/m^2, so that the shading cannot be more excellent than 32% in this study.

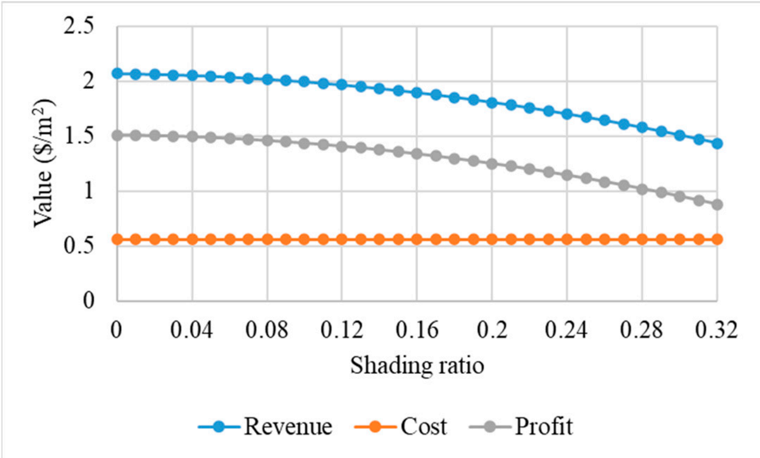

Figure 9. Revenue, cost, and profit of soybean production under different shading ratios.

Figure 10 reveals the total annual revenue, cost, and profit of the agrivoltaic system. The values are a summation between electricity production and crop production (see Figures 8 and 9). In the REC and SMP case, the shading ratio of 0.3 is the best solution, with a profit of USD 1.76/m^2/year. Because of soybean production, the shading ratios between 0.16 and 0.32 have positive profits. In the SMP case, the shading ratio of 0.26 is the best solution, with a USD 1.00/m^2/year profit. Due to the value of SMP, profits are more influenced by soybean sales than those of the REC and SMP cases. In both cases, producing electricity does not increase farmer's profit. Similarly, regarding the fact of a profit of soybean sales only being USD 1.5/m^2/year, the agrivoltaic system was able increase farmers' income to USD 1.76/m^2/year under the REC and SMP case.

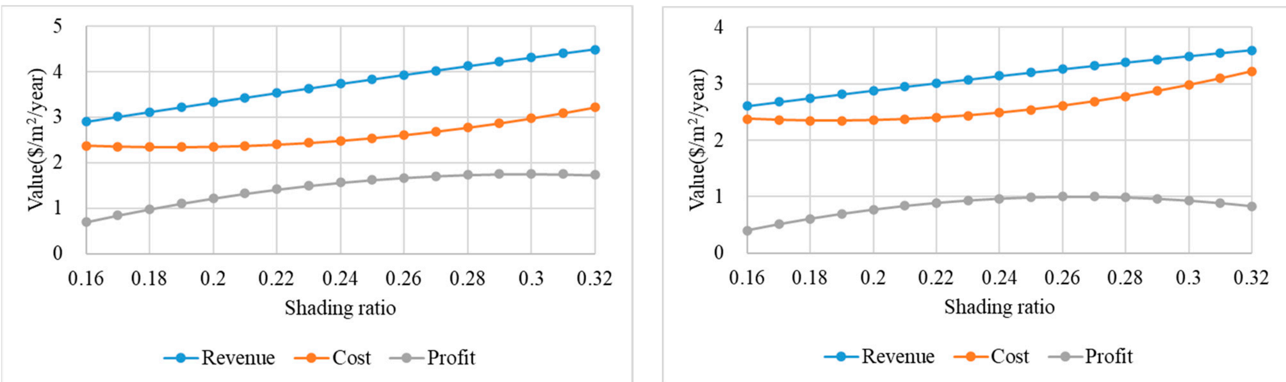

(**a**) (**b**)

Figure 10. Revenue, cost, and profit of the agrivoltaic system: (**a**) REC and SMP case; (**b**) SMP case.

Once the shading ratio of 0.30 is selected, a BIPV can be designed under the agrivoltaic structure shown in Figure 6. Since a semi-transparent BIPV consists of glass and resin, some of solar radiation penetrates BIPVs. It means that the horizontal distance between BIPVs ($e_1 + e_2$) and the area of glass and resin in a semi-transparent BIPV can affect the shading ratio.

Figure 11 shows the design of LG405N2W-V5 with 72 PV cells modifying the semi-transparent BIPV. The devised semi-transparent BIPV consists of 36 PV cells with 202.5 W. Let K_T be a penetration rate of the BIPV, so Equation (11) can be modified as Equation (13).

$$S = (1 - K_T)q/(e_1 + e_2) \tag{13}$$

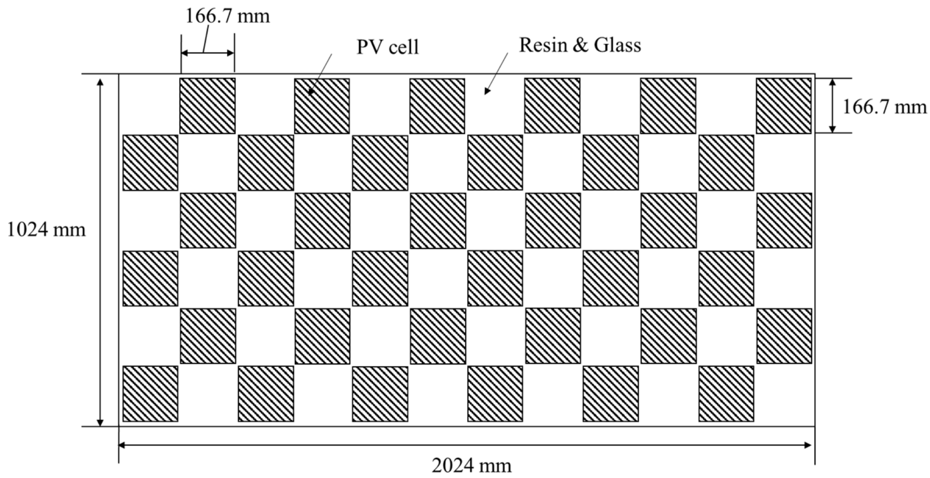

Figure 11. Devised semi-transparent building integrated photovoltaic.

Since $K_T = 0.5$, the horizontal distance between BIPVs can be computed as Equation (14).

$$(e_1 + e_2) = (1 - 0.5) \times 1024/0.3 \cong 1707 \text{ mm} \tag{14}$$

As a result, the subject agrivoltaic system can be designed to maximize its profit from both electricity generation and soybean production.

3.3. Discussion

The study considers soybean production in the subject agrivoltaic system. According to [2], yields of sesame, mung bean, red bean, corn, and soybean under an open field (0% shading ratio) were 0.96, 1.95, 2.35, 8.09, and 3.64 Mg ha^{-1}, respectively, in South Korea. However, at the 21.3% shading ratio condition, sesame, mung bean, red bean, and soybean showed 7%, 21%, 26%, and 13% yield losses, respectively. Interestingly, corn yield increased by 6%. At the 32% shading ratio condition, sesame showed a significant yield loss of 53%, while other crops showed yield losses of 30–44%.

Since soybean showed the average yield reduction trend among the crops, it was selected to demonstrate the proposed design framework of an agrivoltaic system with BIPVs. Notice that most of crops' yields underneath PV modules were reduced. Nevertheless, the agrivoltaic system enabled an increase in the income of farmers because of the revenue from electricity sales. The experiment in Section 3.2 showed that the agrivoltaic system increased farmers' income to USD 1.76/m^2/year under the REC and SMP case when the profit of soybean sales was only USD 1.5/m^2/year. In addition, the shading ratio of 0.3 is the best solution in the REC and SMP case with a profit of USD 1.76/m^2/year. In addition, BIPV is designed to meet a shading ratio of 0.3. As a result, regarding that the profit of an agrivoltaic system is heavily dependent on both REC and SMP prices, sustainable renewable energy policy should be devised to increase farmers' income.

4. Conclusions

This study proposed a framework identifying the optimal design of an agrivoltaic system integrated with a semi-transparent BIPV regarding its economic value. The economic value was estimated based on the performance of an agrivoltaic system in terms of electricity generation and soybean production under different shading ratios. To this end, two estimation models were developed through PR using the data collected from an Agrivoltaic system located at the Jeollanam-do Agricultural Research and Extension Services in Naju-si (35.0161° N, 126.7108° E), Jeollanam-do, South Korea. Under the different shading ratios between 0.16 and 0.32, the optimization model identified the best shading ratio of the agrivoltaic system and devised an appropriate semi-transparent BIPV. In the REC and SMP case, a shading ratio of 0.3 was the best solution, yielding a profit of USD 1.76/m^2/year. A shading ratio of 0.26 was the best solution in the SMP case, yielding a USD 1.00/m^2/profit per year. Consequently, this study shows that the selected shading ratio can be used to design a semi-transparent BIPV with maximum profit. These results will contribute to the implementation of BIPVs in agrivoltaic systems.

Author Contributions: Conceptualization, S.K. (Sojung Kim); methodology, S.K. (Sojung Kim) and S.K. (Sumin Kim); software, S.K. (Sojung Kim); validation, S.K. (Sojung Kim) and S.K. (Sumin Kim); resources, S.K. (Sojung Kim); writing—original draft preparation, S.K. (Sojung Kim) and S.K. (Sumin Kim); writing—review and editing, S.K. (Sojung Kim) and S.K. (Sumin Kim); visualization, S.K. (Sojung Kim); project administration, S.K. (Sojung Kim); funding acquisition, S.K. (Sojung Kim). All authors have read and agreed to the published version of the manuscript.

Funding: This work was supported by the National Research Foundation of Korea (NRF) grant funded by the Korea government (MSIT) (No. 2021R1F1A1045855).

Data Availability Statement: Not applicable.

Conflicts of Interest: The authors declare no conflict of interest.

References

1. Borazan, I.; Bedeloglu, A.C.; Demir, A. A photovoltaic textile design with a stainless steel mesh fabric. *J. Ind. Text.* **2022**, *51*, 1527–1538. [CrossRef]
2. Kim, S.; Kim, S.; Yoon, C.Y. An efficient structure of an agrophotovoltaic system in a temperate climate region. *Agronomy* **2021**, *11*, 1584. [CrossRef]
3. Shukla, A.K.; Sudhakar, K.; Baredar, P. Recent advancement in BIPV product technologies: A review. *Energy Build.* **2017**, *140*, 188–195. [CrossRef]
4. Dimitrijevic, D.; Tomic, M.; Zivkovic, P.; Stojiljkovic, M.; Dobrnjac, M. Thermal characteristics and potential for retrofit by using green vegetated roofs. *Ann. Fac. Eng. Hunedoara* **2016**, *14*, 41.
5. Kim, S.; Kim, S. Economic Feasibility Comparison between Building-Integrated Photovoltaics and Green Systems in Northeast Texas. *Energies* **2023**, *16*, 4672. [CrossRef]
6. Cascone, S. The energy-efficient design of sustainable green roofs in Mediterranean climate: An experimental study. *Energy Build.* **2022**, *273*, 112427. [CrossRef]
7. Debbarma, M.; Sudhakar, K.; Baredar, P. Comparison of BIPV and BIPVT: A review. *Resour.-Effic. Technol.* **2017**, *3*, 263–271. [CrossRef]
8. Yu, G.; Yang, H.; Luo, D.; Cheng, X.; Ansah, M.K. A review on developments and researches of building integrated photovoltaic (BIPV) windows and shading blinds. *Renew. Sustain. Energy Rev.* **2021**, *149*, 111355. [CrossRef]
9. Liu, Z.; Zhang, Y.; Yuan, X.; Liu, Y.; Xu, J.; Zhang, S.; He, B.J. A comprehensive study of feasibility and applicability of building integrated photovoltaic (BIPV) systems in regions with high solar irradiance. *J. Clean. Prod.* **2021**, *307*, 127240. [CrossRef]
10. Gholami, H.; Røstvik, H.N. Economic analysis of BIPV systems as a building envelope material for building skins in Europe. *Energy* **2020**, *204*, 117931. [CrossRef]
11. Grand View Research. Building Integrated Photovoltaics Market Size Report. 2023. Available online: https://www.grandviewresearch.com/industry-analysis/building-integrated-photovoltaics-bipv-market (accessed on 2 April 2023).
12. Chen, F.; Wittkopf, S.K.; Ng, P.K.; Du, H. Solar heat gain coefficient measurement of semi-transparent photovoltaic modules with indoor calorimetric hot box and solar simulator. *Energy Build.* **2012**, *53*, 74–84. [CrossRef]
13. Romaní, J.; Ramos, A.; Salom, J. Review of transparent and semi-transparent building-integrated photovoltaics for fenestration application modeling in building simulations. *Energies* **2022**, *15*, 3286. [CrossRef]
14. Kim, S.; Kim, S. Optimization of the design of an agrophotovoltaic system in future climate conditions in South Korea. *Renew. Energy* **2023**, *206*, 928–938. [CrossRef]
15. Chopard, J.; Bisson, A.; Lopez, G.; Persello, S.; Richert, C.; Fumey, D. Development of a decision support system to evaluate crop performance under dynamic solar panels. In *AIP Conference Proceedings*; AIP Publishing: Melville, NY, USA, 2021; Volume 2361. [CrossRef]
16. Lu, S.M.; Zainali, S.; Stridh, B.; Avelin, A.; Amaducci, S.; Colauzzi, M.; Campana, P.E. Photosynthetically active radiation decomposition models for agrivoltaic systems applications. *Sol. Energy* **2022**, *244*, 536–549. [CrossRef]
17. Beck, M.; Bopp, G.; Goetzberger, A.; Obergfell, T.; Reise, C.; Schindele, S. Combining PV and food crops to Agrophotovoltaic–optimization of orientation and harvest. In Proceedings of the 27th European Photovoltaic Solar Energy Conference and Exhibition, EU PVSEC, Frankfurt, Germany, 24 September 2012.
18. Elborg, M. Reducing land competition for agriculture and photovoltaic energy generation—A comparison of two agro-photovoltaic plants in japan. In Proceedings of the International Conference on Sustainable and Renewable Energy Development and Design (SREDD2017), Thimphu, Bhutan, 3 April 2017.

19. Schindele, S.; Trommsdorff, M.; Schlaak, A.; Obergfell, T.; Bopp, G.; Reise, C.; Braun, C.; Weselek, A.; Bauerle, A.; Högy, P.; et al. Implementation of agrophotovoltaics: Techno-economic analysis of the price-performance ratio and its policy implications. *Appl. Energy* **2020**, *265*, 114737. [CrossRef]
20. Hassanpour Adeh, E.; Selker, J.S.; Higgins, C.W. Remarkable agrivoltaic influence on soil moisture, micrometeorology and water-use efficiency. *PLoS ONE* **2018**, *13*, e0203256. [CrossRef]
21. Alkan, S.; Ates, Y. Pilot Scheme Conceptual Analysis of Rooftop East–West-Oriented Solar Energy System with Optimizer. *Energies* **2023**, *16*, 2396. [CrossRef]
22. Kouloumpis, V.; Kalogerakis, A.; Pavlidou, A.; Tsinarakis, G.; Arampatzis, G. Should photovoltaics stay at home? Comparative life cycle environmental assessment on roof-mounted and ground-mounted photovoltaics. *Sustainability* **2020**, *12*, 9120. [CrossRef]
23. Waller, R.; Kacira, M.; Magadley, E.; Teitel, M.; Yehia, I. Semi-transparent organic photovoltaics applied as greenhouse shade for spring and summer tomato production in arid climate. *Agronomy* **2021**, *11*, 1152. [CrossRef]
24. Fung, T.Y.; Yang, H. Study on thermal performance of semi-transparent building-integrated photovoltaic glazings. *Energy Build.* **2008**, *40*, 341–350. [CrossRef]
25. Asfour, O.S. Solar and shading potential of different configurations of building integrated photovoltaics used as shading devices considering hot climatic conditions. *Sustainability* **2018**, *10*, 4373. [CrossRef]
26. Kim, J.C.; Kim, K.N. Study on the Regional Differences of Optimal Orientation and Tilt Angle for Photovoltaic Systems: Simulations by a System Advisor Model. *New Renew. Energy* **2018**, *14*, 9–20. [CrossRef]
27. Korea Meteorological Administration. Automated Synoptic Observing System (ASOS) Data. Available online: https://data.kma.go.kr/data/grnd/selectAsosRltmList.do?pgmNo=36 (accessed on 20 June 2023).
28. Korea Power Exchange. Today Power Information. Available online: https://www.kpx.or.kr/ (accessed on 20 June 2023).
29. WEUP Power Co., Ltd. Products. Available online: https://www.weuppower.com/ (accessed on 20 June 2023).
30. Pardo, M.Á.; Jodar-Abellan, A.; Vélez, S.; Rodrigo-Comino, J. A method to estimate optimal renovation period of solar photovoltaic modules. *Clean Technol. Environ. Policy* **2022**, *24*, 2865–2880. [CrossRef]
31. Walker, A.; Lockhart, E.; Desai, J.; Ardani, K.; Klise, G.; Lavrova, O.; Tansy, T.; Deot, J.; Fox, B.; Pochiraju, A. *Model of Operation-and-Maintenance Costs for Photovoltaic Systems*; Technical Report No. NREL/TP-5C00-74840; National Renewable Energy Laboratory: Golden, CO, USA, 2020.
32. Sullivan, W.G.; Wicks, E.M.; Koelling, C.P. *Engineering Economy*, 16th ed.; Pearson Higher Education, Inc.: New York, NY, USA, 2013.
33. Korea Agro-Fisheries & Food Trade Corporation. Price Information. Available online: https://www.kamis.or.kr/customer/main/main.do (accessed on 20 June 2023).